

Discussion on Beam Delivery Systems for Advanced Linear Colliders

Spencer Gessner

LCWS2021

March 18th, 2021



U.S. DEPARTMENT OF
ENERGY

Stanford
University

SLAC NATIONAL
ACCELERATOR
LABORATORY

Overview

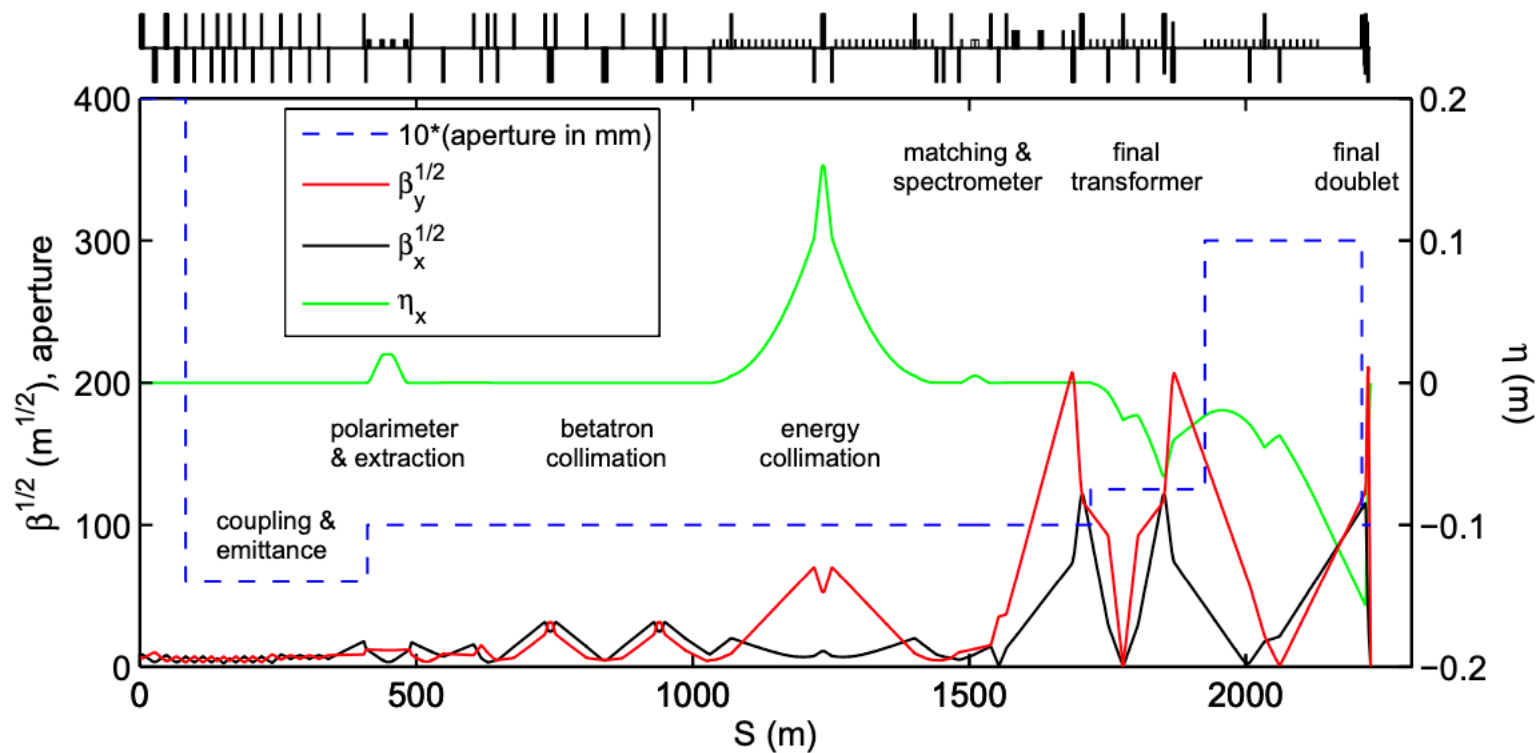
- Ultra-high energy, high luminosity linear colliders require that we reimagine what a Beam Delivery System should do?
- The BDS is accelerator technology independent. It should work with conventional RF technology or advanced accelerator technology.
- The AAC and broader Beam Dynamics communities can come together to study this topic.

Physics Questions

- Can we beat scaling laws based on “traditional” BDS systems?
- Should we consider BDS for both symmetric and flat beams?
- What are the implications of using ultra-short bunches?
- What are the benefits/drawbacks of plasma lens systems?

Technical Questions

- Can we shorten the BDS by incorporating novel diagnostic and collimation systems?
- Do Machine-Detector Interface requirements change if we pursue an energy frontier machine (*i.e.* no longer focus on precision measurements)?
- What are the implications of using plasma lenses near the IP?



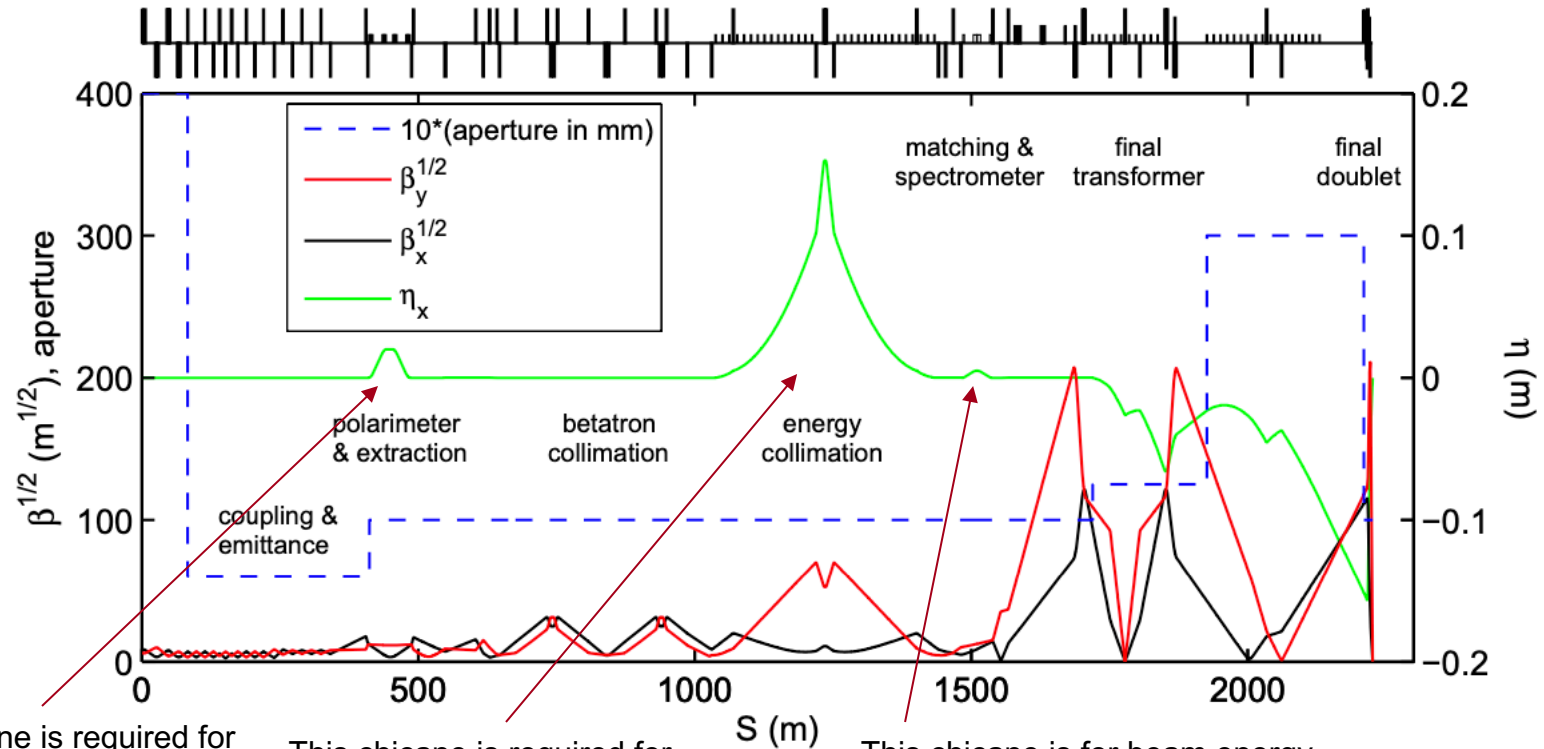
BDS Components

The BDS is composed of:

- Tune-up and diagnostic sections including:
 - Emittance (laser wire)
 - Polarimetry
 - Energy measurement
- Collimation system
 - Design requirement for ILC is ZERO particles lost in final few hundred meters
- Machine protection
- Final focus with local chromaticity correction

What drives the length of the BDS?

Bends are designed to limit emittance growth due to synchrotron radiation below 1%.

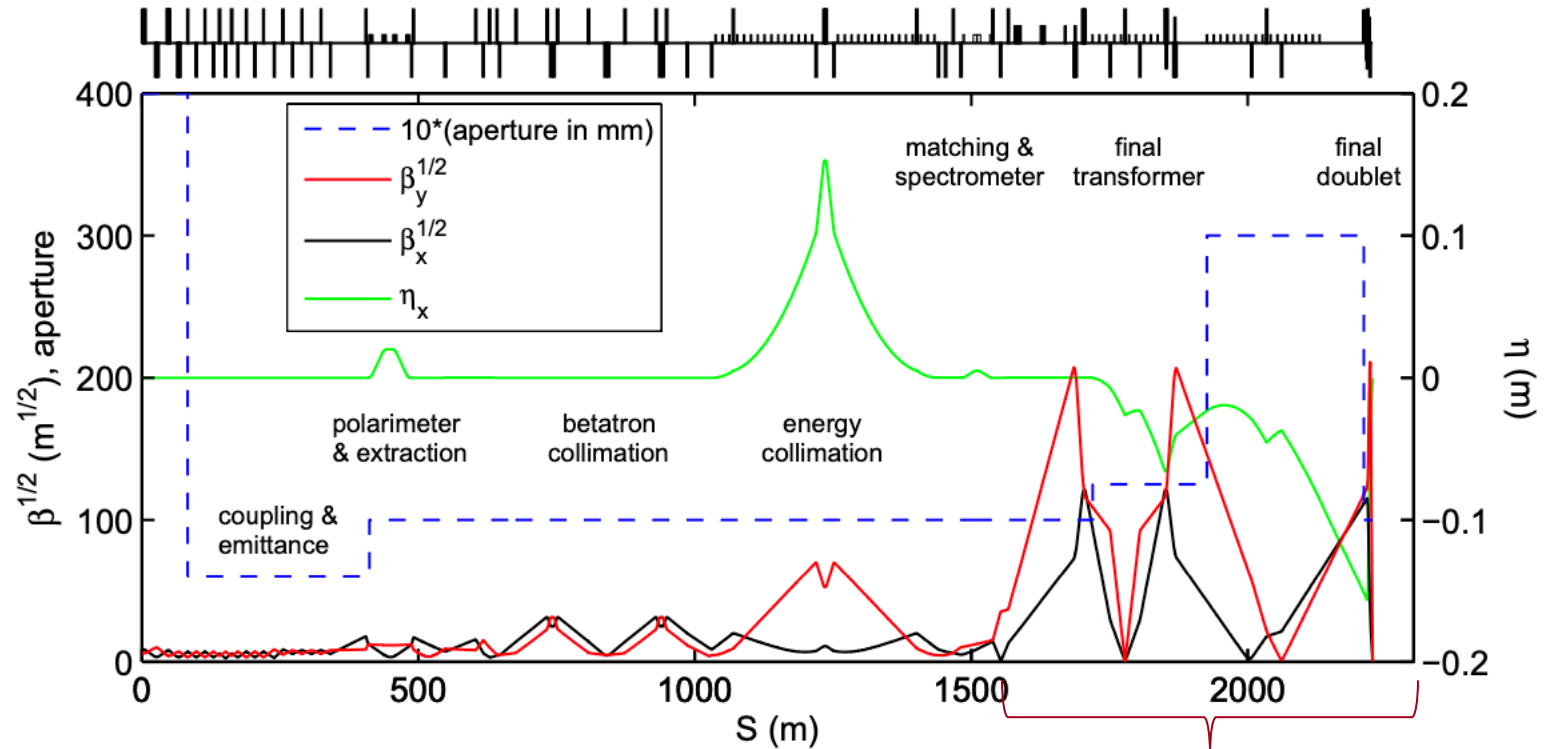


This chicane is required for emittance and polarimetry

This chicane is required for energy collimation

This chicane is for beam energy measurement (1E-4 resolution).

What drives the length of the BDS?



Bends in the final focus system are required for chromatic correction.

Final Focus

Final Focus design comes from paper by [P. Raimondi and A. Seryi, Phys. Rev. Lett, 86, 3779 \(2001\)](#).

System employs “local” chromaticity correction.

The length of the FF system scales as $L \propto \gamma^{7/10}$ where the main consideration is emittance growth due to ISR.

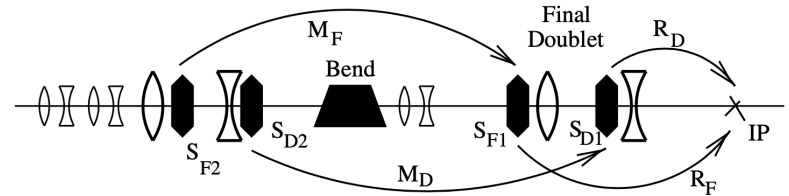


FIG. 2. Optical layout of the new final focus.

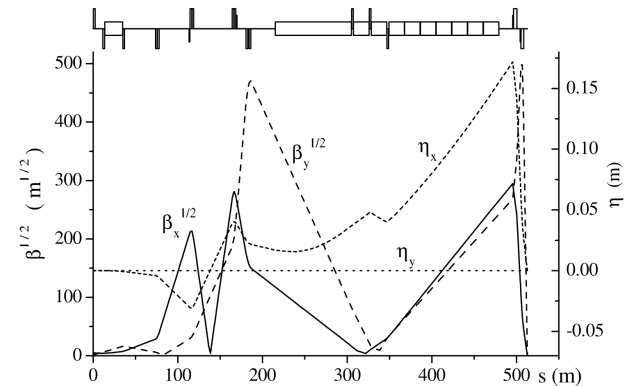


FIG. 3. Optics of the new NLC final focus system showing horizontal and vertical betatron (β) and dispersion (η) functions similarly to Fig. 1.

Oide Limit

Synchrotron radiation limits come from paper by [K. Oide, Phys. Rev. Lett, 61, 1713, \(1988\)](#).

Doesn't matter what type of focusing system is used. Final betafuncion and beam size depends only on emittance.

$$\sigma_{y \min}^* = \left(\frac{7}{5} \right)^{1/2} \left[\frac{275}{3\sqrt{6\pi}} r_e \lambda_e F(\sqrt{KL}, \sqrt{Kl^*}) \right]^{1/7} (\epsilon_{Ny})^{5/7},$$

$$\beta_y^* = \left[\frac{275}{3\sqrt{6\pi}} r_e \lambda_e F(\sqrt{KL}, \sqrt{Kl^*}) \right]^{2/7} \gamma (\epsilon_{Ny})^{3/7}.$$

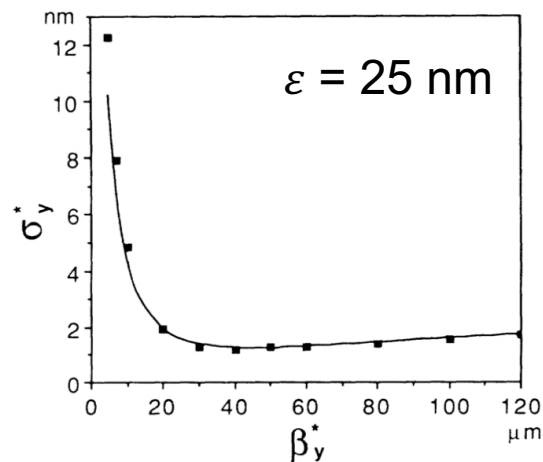


FIG. 2. The beam size as a function of the beta function at the collision point. The solid line is obtained from Eq. (11), and the markers represent the numerical results of a multiparticle tracking simulation with 4000 particles.

Short Bunches for Increased Luminosity

SLAC

We “win” twice by using short bunches.

First, short bunches suppress beamstrahlung, increasing both luminosity and luminosity in 1%.

Second, shorter bunches allow for smaller betafuncions due to hourglass effect.

$$\mathcal{L} = \frac{0.30H_D}{4\pi\alpha^2} \sqrt{\frac{\gamma}{r_e\sigma_z} \frac{n_\gamma^{3/2}}{\sigma_y} \frac{\eta P_{AC}}{\mathcal{E}_b}}$$

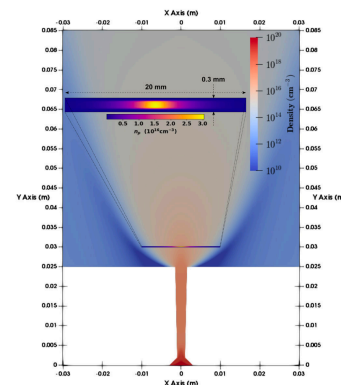
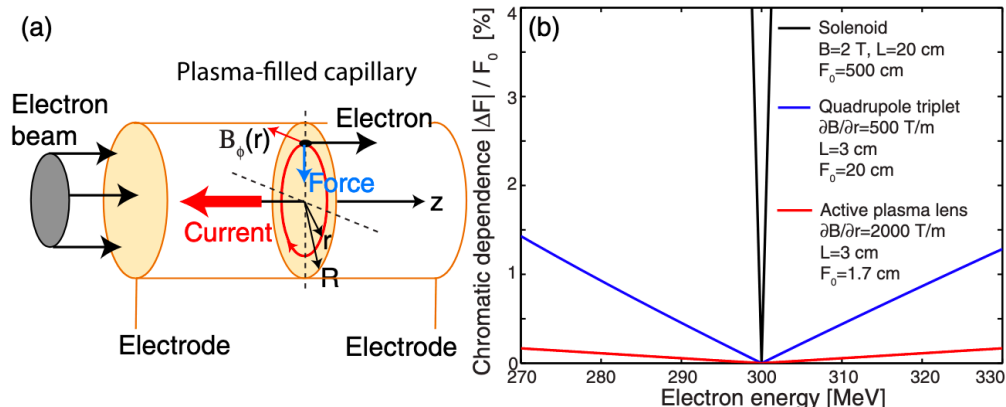
Reduce σ_z from 300 μm to 3 μm .

Plasma Lens Solutions

Plasma lens systems offer two main advantages:

1. Focusing gradients are orders of magnitude larger than what can be achieved with traditional systems.
2. Axisymmetric focusing strongly reduces chromatic effects.

J. van Tilborg et. al., PRL115,184802 (2015)



C. Doss et. al., PRAB 22, 111001 (2019)

Scaling Law's for Emittance Growth

The scaling for emittance growth in the plasma lens is given by:

$$\frac{\partial \varepsilon_n}{\partial z} = \frac{\beta k_p^2 r_e Z}{\gamma} \log \left(\frac{\lambda_D}{R} \right) \propto \frac{\beta n}{\gamma}$$

This holds for unmatched beams in both APLs and PPLs. In APLs, there is additional scattering from plasma electrons but this is assumed to be small compared to the scattering off plasma ions.

$$\Delta \varepsilon \propto \frac{\beta n L}{\gamma}$$

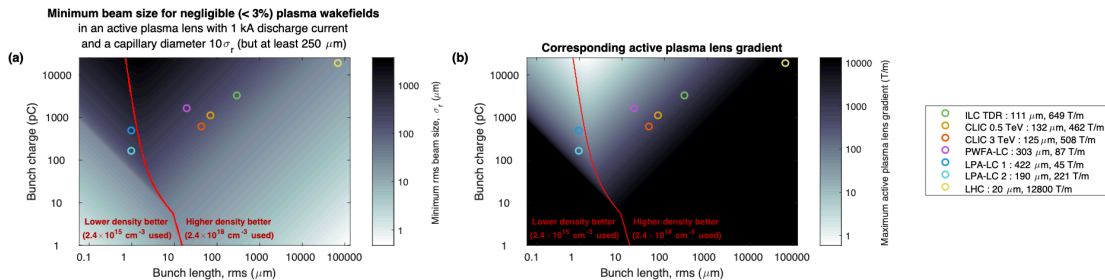
Main point: smaller betas, shorter density-length product, higher energies, limit emittance growth.

Wakefield Limitations in APLs

A study by C. Lindstrom and E. Adli looked at active plasma lenses for Linear Collider final focus systems, with the assumption that the focusing due to the wakefield is much smaller than focusing of the APL.

They find that the beam must have a large transverse size and betafunction when entering the APL.

The large betafunction leads to emittance growth due to scattering in the APL. Snowmass is an excellent forum for examining this issue.



Collider	ILC TDR	CLIC 0.5 TeV	CLIC 3 TeV	PWFA-LC 1 TeV	LP-LC Ex. 1	LP-LC Ex. 2	LHC 13 TeV
Final beam energy (GeV)	250	250	1500	500	500	500	6500
Charge per bunch (pC)	3200	1088	595	1600	480	160	18400
Bunch length, rms (μm)	300	72	44	20	1	1	7.6×10^4
Normalized emittance, x/y ($\mu\text{m rad}$)	10/0.035	2.4/0.025	0.66/0.02	10/0.035	1/0.01	1/0.01	3.75
<i>Considerations for an active plasma lens with 1 kA discharge current and a minimum diameter 250 μm</i>							
Min. beam size for negligible (< 3%) wake (μm)	111	132	125	303	422	190	20
Max. APL gradient with negligible wake (T/m)	649	462	508	87	45	221	12800
Required beta function $\sqrt{\beta_x \beta_y}$, final energy (m)	1.0×10^4	3.5×10^4	4.0×10^5	1.5×10^5	1.7×10^6	3.5×10^5	0.74

C. Lindstrom, E. Adli, "Analytic plasma wakefield limits for active plasma lenses" [arXiv:1802.02750], 2018.

Beating the Oide Limit

In the paper by [Chen et. al.](#), they propose to beat Oide limit by making the beam radiate in the quantum regime.

This solutions requires that the beam be made as small as possible at the entrance of the plasma lens.

VOLUME 64, NUMBER 11

PHYSICAL REVIEW LETTERS

12 MARCH 1990

Plasma-Based Adiabatic Focuser

P. Chen and K. Oide^(a)

Stanford Linear Accelerator Center, Stanford University, Stanford, California 94309

A. M. Sessler

Lawrence Berkeley Laboratory, Berkeley, California 94720

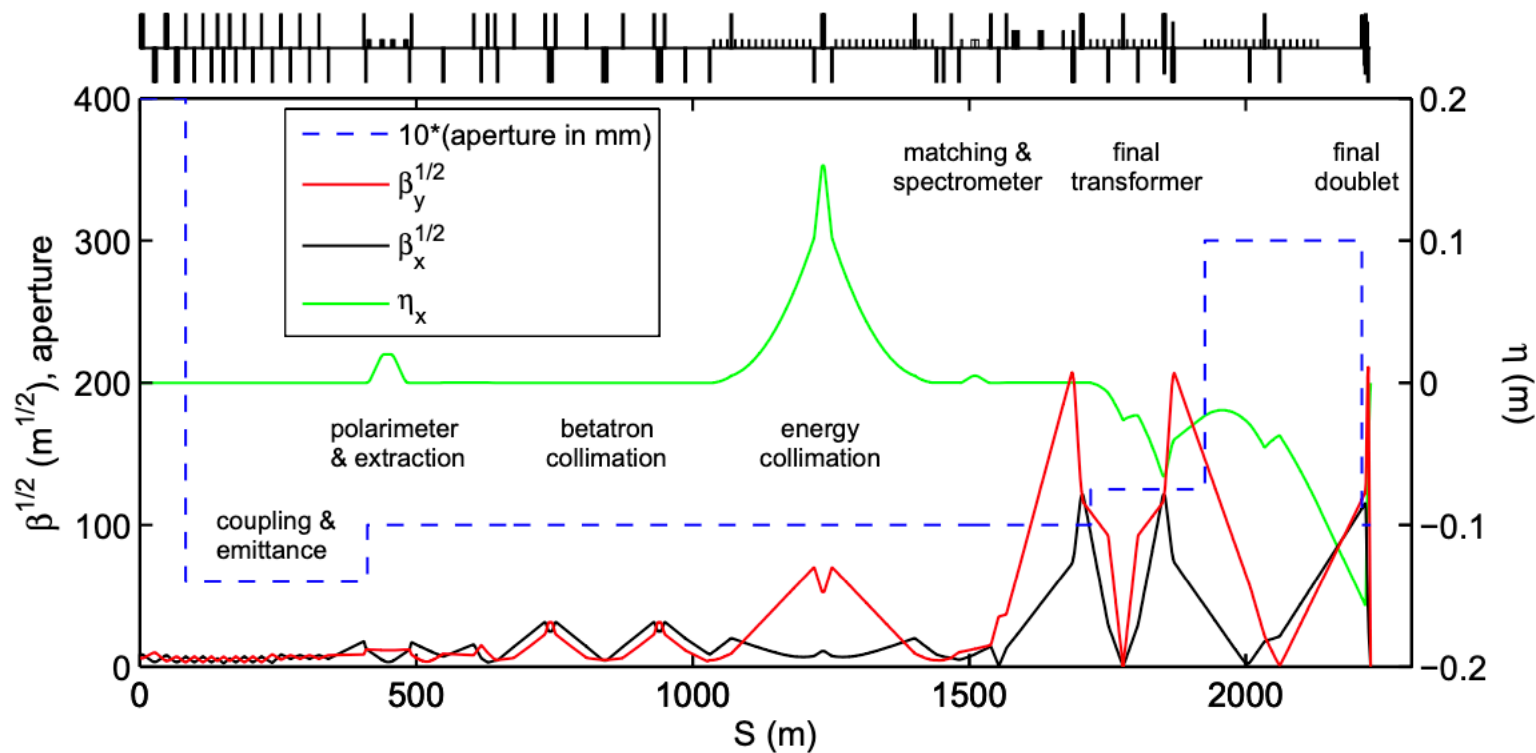
S. S. Yu

Lawrence Livermore National Laboratory, P.O. Box 808, Livermore, California 94550

(Received 30 October 1989)

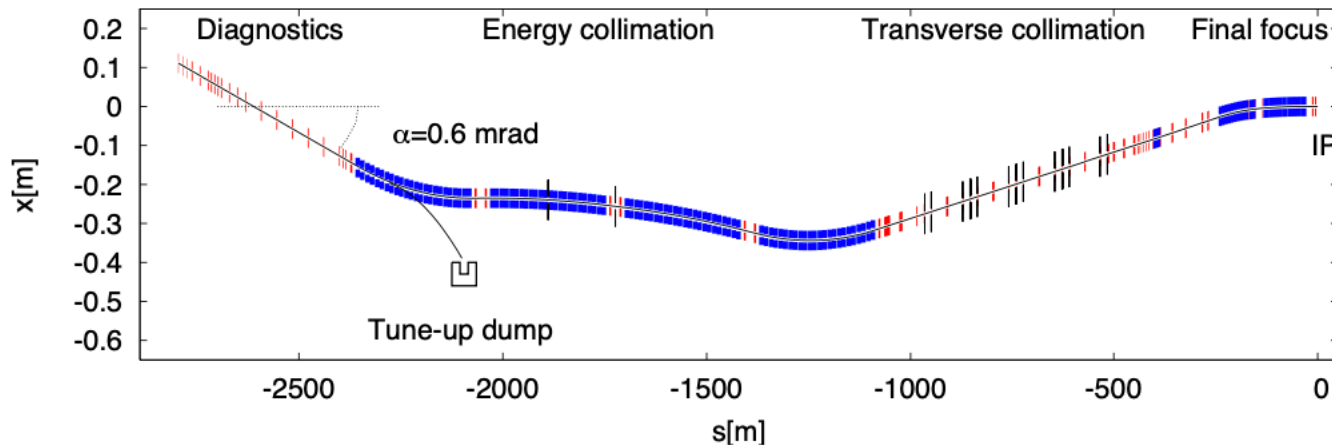
Theoretical analysis is made of an intense relativistic electron beam moving through a plasma of increasing density, but density always less than that of the beam (underdense). Analysis is made of the beam radiation energy loss and it is noted that the focuser is insensitive to the beam energy spread due to radiation loss. Furthermore, because of the scaling behavior in the nonclassical regimes, the radiation limit on lenses (the Oide limit) can be exceeded.

$$\sigma_q \gg \left[\frac{1}{22} \lambda_c \epsilon_n^2 (1 + \alpha_0^2) \right]^{1/3} \\ \times \exp \left[-3 \left(\frac{\alpha_0^3}{(1 + \alpha_0^2)^2} \frac{\lambda_c}{\alpha^3 \epsilon_n} \right)^{1/3} \right]$$



Parameter		Center-of-mass energy, E_{cm} (GeV)							Unit
		Baseline				Upgrades			
		200	250	350	500	500	1000 (A1)	1000 (B1b)	
Nominal bunch population	N	2.0	2.0	2.0	2.0	2.0	1.74	1.74	$\times 10^{10}$
Pulse frequency	f_{rep}	5	5	5	5	5	4	4	Hz
Bunches per pulse	N_{bunch}	1312	1312	1312	1312	2625	2450	2450	
Nominal horizontal beam size at IP	σ_x^*	904	729	684	474	474	481	335	nm
Nominal vertical beam size at IP	σ_y^*	7.8	7.7	5.9	5.9	5.9	2.8	2.7	nm
Nominal bunch length at IP	σ_z^*	0.3	0.3	0.3	0.3	0.3	0.250	0.225	mm
Energy spread at IP, e^-	$\delta E/E$	0.206	0.190	0.158	0.124	0.124	0.083	0.085	%
Energy spread at IP, e^+	$\delta E/E$	0.190	0.152	0.100	0.070	0.070	0.043	0.047	%
Horizontal beam divergence at IP	θ_x^*	57	56	43	43	43	21	30	μrad
Vertical beam divergence at IP	θ_y^*	23	19	17	12	12	11	12	μrad
Horizontal beta-function at IP	β_x^*	16	13	16	11	11	22.6	11	mm
Vertical beta-function at IP	β_y^*	0.34	0.41	0.34	0.48	0.48	0.25	0.23	mm
Horizontal disruption parameter	D_x	0.2	0.3	0.2	0.3	0.3	0.1	0.2	
Vertical disruption parameter	D_y	24.3	24.5	24.3	24.6	24.6	18.7	25.1	
Energy of single pulse	E_{pulse}	420	526	736	1051	2103	3409	3409	kJ
Average beam power per beam	P_{ave}	2.1	2.6	3.7	5.3	10.5	13.6	13.6	MW
Geometric luminosity	L_{geom}	0.30	0.37	0.52	0.75	1.50	1.77	2.64	$\times 10^{34} \text{ cm}^{-2} \text{ s}^{-1}$
– with enhancement factor		0.50	0.68	0.88	1.47	2.94	2.71	4.32	$\times 10^{34} \text{ cm}^{-2} \text{ s}^{-1}$
Beamstrahlung parameter (av.)	Υ_{ave}	0.013	0.020	0.030	0.062	0.062	0.127	0.203	
Beamstrahlung parameter (max.)	Υ_{max}	0.031	0.048	0.072	0.146	0.146	0.305	0.483	
Simulated luminosity (incl. waist shift)	L	0.56	0.75	1.0	1.8	3.6	3.6	4.9	$\times 10^{34} \text{ cm}^{-2} \text{ s}^{-1}$
Luminosity fraction within 1%	$L_{1\%}/L$	91	87	77	58	58	59	45	%
Energy loss from BS	δE_{BS}	0.65	0.97	1.9	4.5	4.5	5.6	10.5	%
e^+e^- pairs per bunch crossing	n_{pairs}	45	62	94	139	139	201	383	$\times 10^3$
Pair energy per B.C.	E_{pairs}	25	47	115	344	344	1338	3441	TeV

CLIC BDS



Parameter	Units	Value
Length (linac exit to IP distance)/side	m	2750
Maximum energy/beam	TeV	1.5
Distance from IP to first quad, L*	m	3.5
Crossing angle at the IP	mrad	20
Nominal core beam size at IP, σ^* , x/y	nm	45/1
Nominal beam divergence at IP, θ^* , x/y	μ rad	7.7/10.3
Nominal beta-function at IP, β^* , x/y	mm	10/0.07
Nominal bunch length, σ_z	μ m	44
Nominal disruption parameters, x/y		0.15/8.4
Nominal bunch population, N		3.7×10^9
Beam power in each beam	MW	14
Preferred entrance train to train jitter	σ	< 0.2
Preferred entrance bunch to bunch jitter	σ	< 0.05
Typical nominal collimation aperture, x/y	σ_x/σ_y	15/55
Vacuum pressure level, near/far from IP	10^{-9} mbar	1000/1